ASTONJADRO

pISSN 2302-4240
eISSN 2655-2086

Volume 14, Issue 4, December 2025, pp.01273-01285
DOI: http://dx.doi.org/10.32832/astonjadro.v14i4.19246 http://ejournal.uika-bogor.ac.id/index.php/ASTONJADRO

Numerical Simulation of RC Beam-Column Joint: Influence of Discrete Crack Modeling on Hysteresis Response

Brihaspati, Ashar Saputra, Angga Fajar Setiawan

Department of Civil and Environmental Engineering, Universitas Gadjah Mada, Yogyakarta, INDONESIA

E-mail: saputra@ugm.ac.id

| Submitted: March 01, 2025 | Revised: May 02, 2025 | Accepted: August 11, 2025 |

| Published: December 31, 2025 |

ABSTRACT

Understanding the hysteresis behavior of reinforced concrete (RC) beam-column joints with monolithic slabs under cyclic loading is essential for assessing seismic performance. Finite element analysis (FEA) provides a powerful tool for such studies, but accurately capturing cyclic response remains challenging. This research aims to develop and validate an FEA model that provides the hysteresis behavior of an RC beam-column joint focusing on material modeling approaches and emphasizing the influence of discrete crack modeling in simulating major crack opening and closure. The numerical model is implemented in ABAQUS/Standard, combining the Concrete Damaged Plasticity (CDP) model for concrete, combined hardening for reinforcement, and discrete crack representation to enhance crack behavior simulation. The model is validated against previous experimental results by [9] under the same cyclic loading protocol. The results show that least one discrete crack significantly enhances the agreement between numerical and experimental hysteresis loops, while two discrete cracks provide the best match for capturing pinching effect and cyclic stiffness degradation. The compression stiffness recovery parameter (w_c) in CDP and the combined hardening model for reinforcement also play critical roles in influencing numerical results. The model successfully reproduces cyclic stiffness degradation and energy dissipation, although minor discrepancies exist due to material data limitations. This study advances numerical modeling of RC beam-column joints under cyclic loading, emphasizing the importance of discrete crack modeling in enhancing simulation accuracy for seismic performance assessment.

Keywords: beam-column, cyclic, hysteresis, ABAQUS, discrete crack.

INTRODUCTION

The behavior of reinforced concrete (RC) beam-column joints plays a crucial role in the seismic performance of structures. Under cyclic loading, these joints experience progressive stiffness degradation, strength deterioration, and pinching effects. Hysteresis loops serve as a key tool in studying these behaviors, offering valuable insights into degradation mechanisms. While extensive experimental studies have provided critical data on failure modes, energy dissipation, and stiffness degradation, such research is often limited by high costs, time constraints, and challenges in capturing internal stress states and damage evolution. To address these limitations, numerical modeling has become an essential approach, complementing experimental findings and providing a deeper understanding of RC structures under cyclic loading.

Numerous studies have been carried out to better understand the behavior of RC beam-column joints. Experimental and analytical investigations into substandard beam-column joints highlight critical design deficiencies, such as insufficient rebar anchorage, inadequate lap splices, and lack of joint confinement. These deficiencies lead to premature bond-slip failure, excessive rebar pullout, and reduced energy dissipation, ultimately increasing collapse risk. Unconfined joints experience severe shear failure, while short lap splices limit column flexural strength, dominating the failure mechanism despite additional reinforcement [12]. Research on partially debonded longitudinal rebars (PDLRs) indicates that PDLR specimens develop wider cracks with deformation primarily governed by bond-slip, whereas non-PDLR specimens exhibit higher stiffness with flexural-dominated deformation [22]. The influence of stirrups and concrete strength in RC exterior beam-column joints has also been examined, showing that while stirrups enhance displacement capacity

and shear resistance in later loading stages, concrete strength plays a more significant role in shear capacity and crack behavior under cyclic loading [4]. Numerical simulations using ABAQUS have identified concrete strength as the most critical factor affecting shear stress and strain in beam-column joints. A higher joint aspect ratio improves shear strength by delaying diagonal cracking, whereas beam reinforcement has minimal impact [8]. Further numerical investigation of RC exterior beam-column joints under cyclic loading has shown that cracks predominantly form at the beam-joint interface, resulting a flexural hinge. Crossed inclined bars and stirrups enhance structural performance, while variations in stirrup spacing and tie configurations have little effect on overall strength. Increasing beam flexural reinforcement improves load-displacement behavior, with an optimal reinforcement ratio of 0.4% [19]. Meanwhile, in RC exterior beam-column joint with monolithic slab, the slab significantly influences strength, stiffness, and energy dissipation. It increases the negative moment capacity of beams by up to 70%, and neglecting this contribution may lead to strength underestimation and premature column hinging. Under cyclic loading, the slab enhances both strength and stiffness; however, stiffness degradation is more pronounced when the slab is in compression [9].

In this study, a finite element model (FEM) of a RC beam-column joint with monolithic slab is developed in ABAQUS to simulate its behavior under cyclic loading. The model is based on the experimental setup by [9] , ensuring a realistic representation of joint performance. The Concrete Damage Plasticity (CDP) model is applied to simulate behavior of concrete material, capturing stiffness degradation and plastic deformation. However, directly applying the CDP model often leads to inaccuracies in capturing the crack opening and closing behavior of reinforced concrete under cyclic loading. The CDP model, formulated using plasticity theory and damage mechanics within a continuum mechanics framework [14], simulates concrete cracking through plastic strain accumulation rather than explicitly modeling crack formation. As a result, this approach causes a noticeable drift in the recompression branch following tensile unloading and produces overly rounded hysteresis loops, leading to an overestimation of energy dissipation ([21], [23]. To address these shortcomings, [6] introduced a discrete crack method, later refined by [10], [11], which enables the explicit simulation of macro-crack propagation, allowing for a more accurate representation of pinching effects, stiffness degradation, and cyclic behavior in RC structures. Additionally, reinforcement bars are modeled as truss elements with combined hardening properties, ensuring a realistic simulation of rebar plasticity and the Bauschinger effect. The accuracy of the numerical model in capturing the hysteresis response of an RC beam-column joint is validated through a comparison with experimental data.

Existing FEM studies often fail to accurately capture key nonlinear behaviors, such as stiffness degradation and the pinching effect, while the lack of extensive validation against experimental data further reduces their reliability. Addressing these gaps, this study aims to develop a validated and comprehensive numerical model that can represents the hysteresis behavior of RC beam-column joints with monolithic slabs under cyclic loading. The model's reliability and relevance for seismic design will be ensured through validation against experimental data from [9]. Additionally, the study evaluates the effect of discrete cracks and investigates the influence of material modeling approaches, including the stiffness recovery parameter in the CDP model and rebar hardening. The findings contribute to improving numerical methodologies for seismic performance assessment, bridging the gap between numerical modeling and experimental observations.

RESEARCH METHODS

Research Workflow

In this study, a finite element model of an exterior reinforced concrete (RC) beam-column joint with monolithic slab is developed in ABAQUS, based on experimental configuration established by [9]. Figure 1 provides a comprehensive summary of the research workflow, highlighting the key steps from experimental data extraction to numerical simulation and result validation.

pISSN 2302-4240
eISSN 2655-2086
Volume 14, Issue 4, December 2025, pp.01273-01285
DOI: http://dx.doi.org/10.32832/astonjadro.v14i4.19246 http://ejournal.uika-bogor.ac.id/index.php/ASTONJADRO

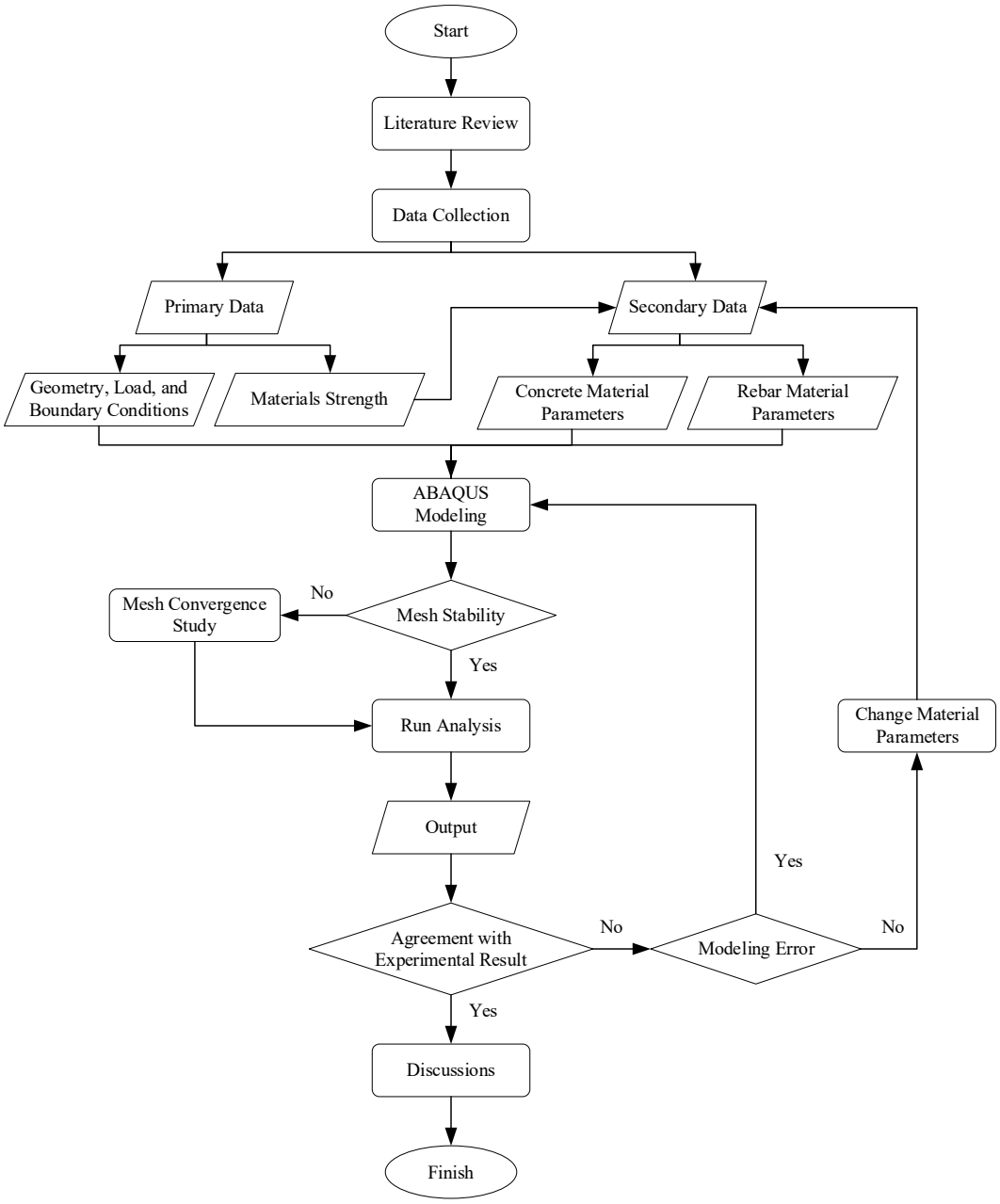

Figure 1. Research flowchart

Geometry and Mesh

The model geometry is developed according to the experimental study by [9]. The column features a square cross-section measuring 304.8 mm, with solid elastic steel supports modeled at both the top and bottom ends to simulate boundary conditions effectively. The longitudinal beam has a cross-section of 254×381 mm and a length of 1.676 m, while transverse beams, each with a cross-section of 254×381 mm, are positioned on two opposite sides of the column. The monolithic reinforced concrete slab has a thickness of 101.6 mm. To mitigate damage concentration at critical boundary regions due to load application and constraints, the concrete regions at the beam ends and both column ends were modeled using an elastic concrete material. The reinforcement details consist of #8 bars for the column longitudinal reinforcement and #6 bars for the beam longitudinal

reinforcement. The detailed dimensions and reinforcement configuration of the model are provided in Figure 2 and Figure 3.

For the numerical simulation, the concrete is modeled using an 8-node linear brick element with reduced integration (C3D8R), while the reinforcement steel is represented by a 2-node linear 3D truss element (T3D2). The mesh size was determined through a convergence study, as shown in Figure 4, to achieve a balance between computational efficiency and result accuracy. The solid elements have a size of 40 mm, while the truss elements measure 20 mm. A finer mesh was applied in the critical region of the beam near the column face to improve the accuracy of stress and strain distribution, as plastic hinges were expected to form in this area. As a result, the model consists of 21,163 solid elements, including the refined mesh, and 5,493 truss elements, leading to a total of 26,656 elements. The simulation is performed using the ABAQUS/Standard solver under cyclic loading conditions.

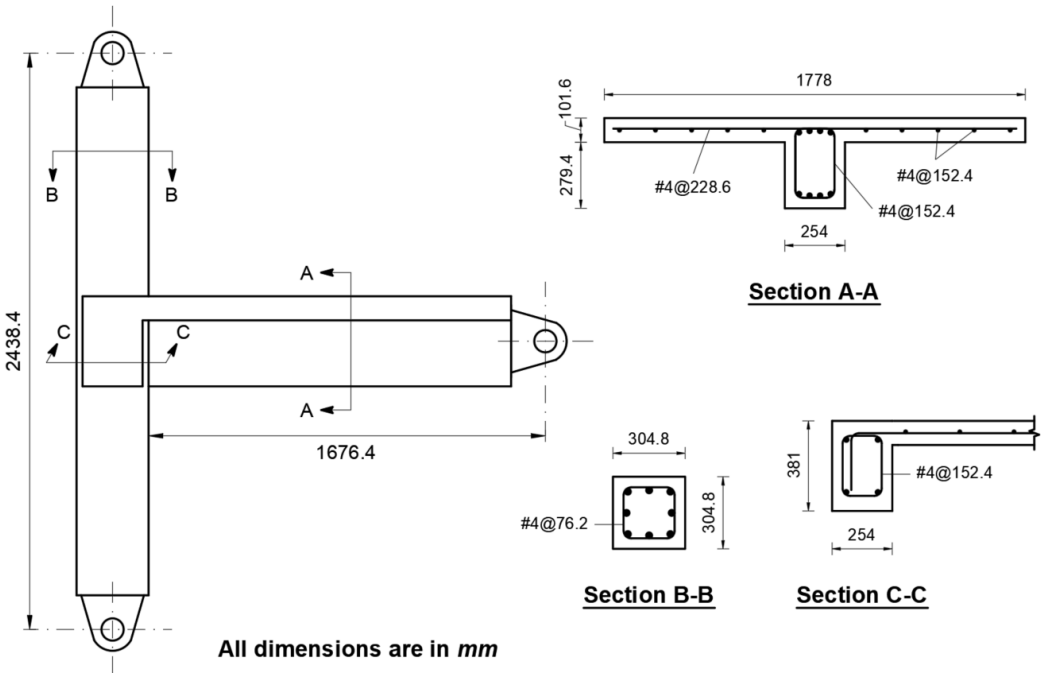

Figure 2. Dimensions and reinforcement configuration [9]

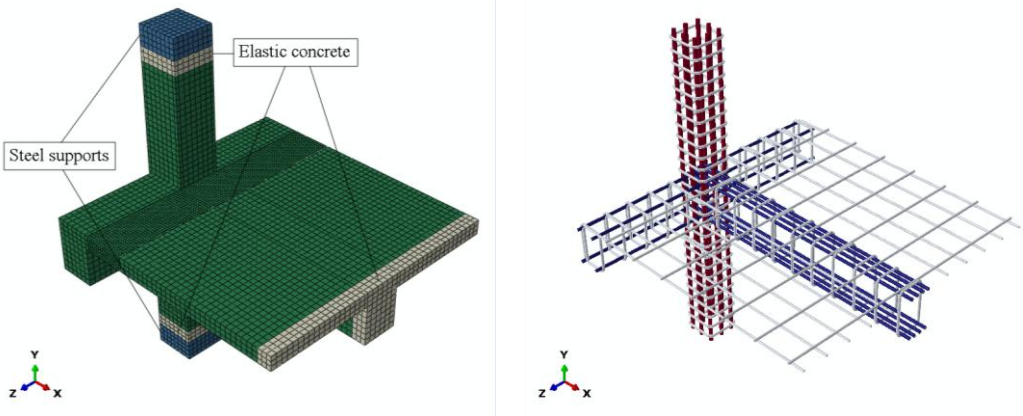

(a) Solid elements (b) Truss elements

Figure 3. Finite element representations

pISSN 2302-4240
eISSN 2655-2086
Volume 14, Issue 4, December 2025, pp.01273-01285
DOI: http://dx.doi.org/10.32832/astonjadro.v14i4.19246 http://ejournal.uika-bogor.ac.id/index.php/ASTONJADRO

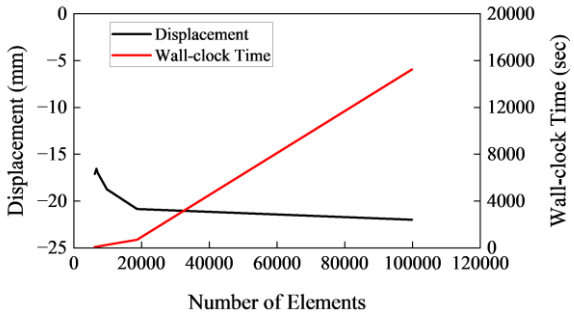

Figure 4. Mesh convergence study

Concrete Material Properties

The Mander constitutive model [17] is adopted to define the stress-strain relationship of concrete in compression, as it effectively represents the nonlinear behavior of concrete. Meanwhile, the tensile stress-strain behavior is modeled using a bilinear constitutive model, considering the significantly lower tensile strength of concrete compared to its compressive strength. The compressive strength of concrete used in this study is based on experimental data, which reported a value of 40.71 MPa [9]. The stress-strain relationship for the concrete material is shown in Figure 5.

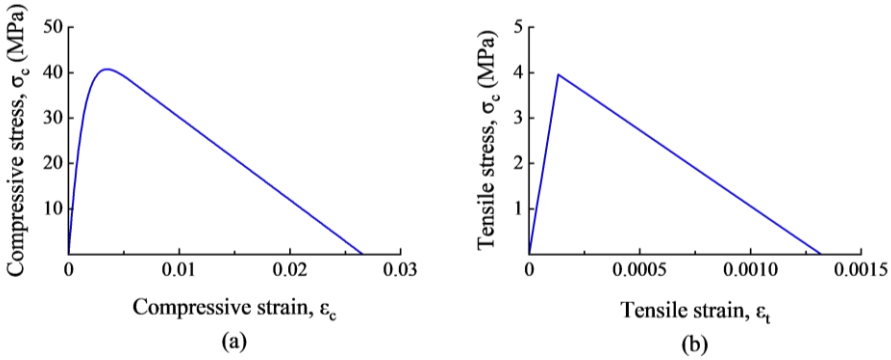

Figure 5. Concrete uniaxial behavior: (a) Compressive stress-strain relation and (b) Tensile stress-strain relation

The CDP model is employed to represent the plastic behavior of concrete. This model combines plasticity theory with damage mechanics, utilizing the formulation introduced by [16] and later enhanced by [14]. Furthermore, the yield function is based on a modified Drucker-Prager hyperbolic equation. In this study, the parameter K_c is set to the default value of 2/3 in ABAQUS, which defines the ratio between the second stress invariant on the tensile meridian and the compressive meridian within the deviatoric plane for concrete. Regarding the dilation angle, previous studies ([3], [5], [15] typically assume a value of approximately 30°, while in this study, a dilation angle of 38° is adopted based on relevant references in the literature [20]. In addition, experimental data support the establishment of the ratio of biaxial to uniaxial compressive yield stresses at 1.16 [13]. Lastly, the viscosity parameter is assigned a small value to ensure convergence with experimental results, particularly in the post-peak softening region [7]. For this research, a viscosity value of 0.0005 is used.

The CDP model defines two primary concrete failure mechanisms, including tensile cracking and compressive crushing. The development of the yield or failure surface is controlled by two hardening parameters, $\tilde{\varepsilon}_t^{pl}$ and $\tilde{\varepsilon}_c^{pl}$ which refer to tensile and compressive equivalent plastic strains, respectfully. These variables correspond to failure mechanisms under tensile and compressive loading. In uniaxial cyclic loading, the degradation of tangent stiffness in concrete is influenced by the unilateral effect, also referred as stiffness recovery. This phenomenon describes the partial restoration of elastic stiffness when the load direction reverses during cyclic loading. The CDP

model captures this behavior by introducing a scalar damage variable d, which governs the reduction of the elastic modulus throughout the loading process.

$$E = (1 - d)E_0 \tag{1}$$

With E_0 represents the initial (undamaged) modulus of the material, E is the reduced tangent stiffness, and d is the scalar damage variable, a function of the stress state and the damage variables for compression (d_c) and tension (d_t). Abaqus assumes that:

$$(1 - d) = (1 - s_t d_c)(1 - s_c d_t) \tag{2}$$

Where s_t and s_c are coefficients associated with the stress state function and stiffness recovery effect, defined as:

$$s_t = 1 - w_t r^*(\sigma_{11}); \ \ 0 \le w_t \le 1 \tag{3}$$

$$s_c = 1 - w_c\big(1 - r^*(\sigma_{11})\big); \ \ 0 \le w_c \le 1 \tag{4}$$

σ_{11} represents the first principal uniaxial stress, r^* is the stress state parameter defined as 1 for tension and 0 for compression [7]. As shown in Figure 6, w_c and w_t represent the factors corresponding to the conditions after tension-compression reversal (w_c) and compression-tension reversal (w_t). During the compression-tension reversal phase, crushed concrete does not experience any recovery, thus w_t is set to 0 [1], [2]. However, during the tension-compression reversal phase, cracks may partially close, recovering some stiffness in compression, though full recovery is not achieved. In the RC beam-column model, damage to the concrete is typically greater near the joint rather than at mid-span. Therefore, w_c = 0.5 is assumed, representing a 50% recovery of the stiffness in compression after cracks close, with the linear damage evolution model used to represent the material strength degradation in both tension and compression.

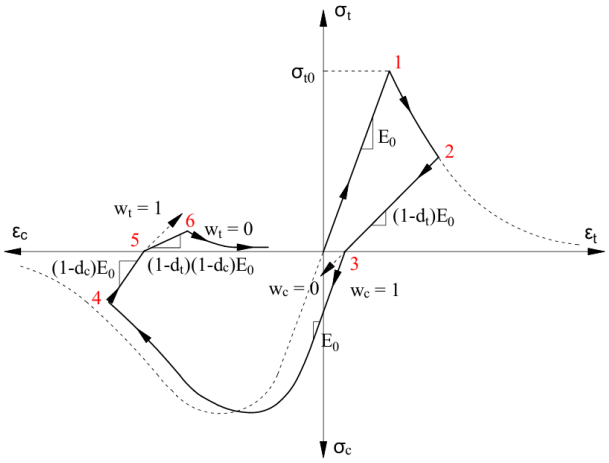

Figure 6. Uniaxial load cycle with different stiffness recovery factors [7]

Rebar Material Properties

Since the model is subjected to cyclic loading, the reinforcing bar material is modeled using a nonlinear combined hardening model. Combined hardening models the Bauschinger effect through kinematic hardening, which translates the yield surface, and strain hardening through isotropic hardening, which expands the yield surface, capturing the material's cyclic plasticity under loading and unloading cycles. The combined hardening model in ABAQUS incorporates parameters from both hardening mechanisms, namely the yield stress at zero plastic strain (f_y), the number of backstresses, the kinematic hardening modulus (C_1), the saturation rate of kinematic hardening (γ_1), the saturated increase in yield stress (Q_∞), and the saturation rate of isotropic hardening (b). These parameters can be determined through experimental testing. In this study, the yield stress value was taken from [9], while the other parameters were adopted from previous study [18], who conducted

pISSN 2302-4240
eISSN 2655-2086
Volume 14, Issue 4, December 2025, pp.01273-01285
DOI: http://dx.doi.org/10.32832/astonjadro.v14i4.19246 http://ejournal.uika-bogor.ac.id/index.php/ASTONJADRO

experimental investigations on the low-cycle fatigue behavior of mild steel and calibrated the cyclic plasticity model using nonlinear combined hardening. The adopted values are presented in Table 1.

Table 1. Combined hardening parameters

Bar size	Yield stress at $\varepsilon^{pl} = 0$ (MPa)	No. of backstresses	C_1 (MPa)	γ_1	Q_∞ (MPa)	b
#4	531.3	1	296717	4815	132	122
#6	414	1	5000	140	180	7
#8	483	1	2220	25	81	5.7

Macro Discrete Crack

The CDP model is widely used to simulate the nonlinear behavior of reinforced concrete. However, it is unable to capture the pinching effect in hysteresis loops, which arises due to material degradation mechanisms such as aggregate interlock loss, bond-slip between reinforcement and concrete, and crack opening and closure. This limitation occurs because the CDP model represents concrete cracking only through plastic strain accumulation rather than explicitly modeling the crack. To more accurately capture pinching behavior, a discrete crack model, originally proposed by [6] and later refined by [10], [11], can be employed. In this approach, macro-cracks are explicitly simulated at region where the tensile demand exceeds the tensile resistance of plain concrete, leading to a more realistic hysteresis response in cyclic loading simulations.

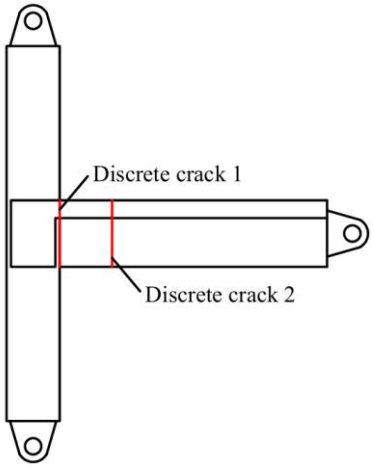

Figure 7. Discrete crack locations

The discrete crack locations are determined through an iterative process. First, an initial trial analysis is conducted without discrete cracks to identify regions experiencing significant tensile damage. The first discrete crack is then introduced in these regions, followed by a second trial analysis to identify additional crack locations. This process is repeated until a stable, non-divergent hysteresis response is achieved. The locations of discrete cracks are illustrated in Figure 7. The first crack occurs at the interface between the beam and column, while the second crack forms 300 mm away from the first crack.

Interactions, Boundary Conditions, and Loading Schemes

The interaction between the rebars and concrete is implemented using an embedded region, where the rebars are embedded within the concrete elements. This ensures that the forces from the rebars are directly transferred to the concrete, enabling a more effective modeling of the material interaction. This approach eliminates the need to define surface contact separately, simplifying the calculation of forces between the materials. Regarding load application, a reference point is defined to impose the displacement-controlled load. This reference point is connected to the surface of the

end beam through kinematic coupling, ensuring that the end beam surface experiences the same displacement as the reference point, thus ensuring uniform load distribution.

To ensure consistency between the numerical model and the experimental conditions, boundary conditions are carefully applied. The upper free-end column has constraints that prevent translations in the U1, U2, and U3 directions on the mid-line of the surface, effectively fixing the position of the upper column. For the lower free-end column, boundary conditions are applied to restrain only the U1 and U3 translations along the mid-line of the surface as shown in Figure 8. Cyclic loading is applied at the free end of the beam. The cyclic loading is applied using displacement control, with the cyclic loading protocol presented in Figure 9.

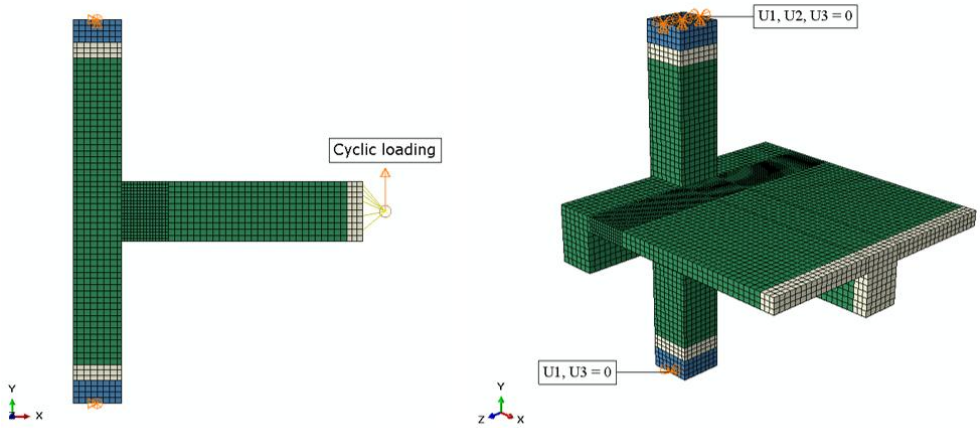

Figure 8. Load and boundary conditions

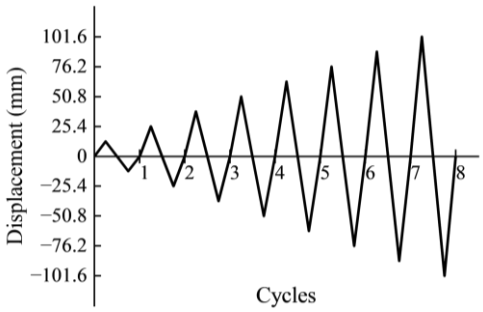

Figure 9. Cyclic loading protocol [9]

RESULT AND DISCUSSION

This section presents the numerical results of the developed finite element model and compares them with the experimental data. The discussion focuses on the hysteresis behavior of the RC beam-column joint with a monolithic slab, specifically examining the influence of discrete crack modeling. The accuracy of the numerical model is assessed by comparing the simulated and experimental hysteresis loops. Additionally, the limitations of the model are addressed to provide insights for future research.

Influence of Macro Discrete Cracks

The hysteresis loops presented in Figure 10 illustrate the effect of incorporating macro discrete cracks in the numerical model on the cyclic response of the exterior beam-column joint. Three different configurations were analyzed: (i) model without discrete cracks, (ii) model with a single discrete crack, and (iii) model with two discrete cracks.

In the model without discrete cracks (left), the hysteresis loop exhibits a smooth, nearly perfect shape with no visible pinching effects. This indicates an overestimation of the energy dissipation capacity,

as the model does not account for localized damage and crack-induced stiffness degradation. This limitation arises because the CDP model, in its standard form, does not explicitly capture the opening and closing of cracks, which are key contributors to the pinching effect. In contrast, the model with a single discrete crack (center) already captures the pinching effect under lateral loading, representing the progressive loss of stiffness due to crack formation and slip along the crack interface. The most significant improvement is observed in the model with two discrete cracks (right), where the pinching effect is well captured, and the hysteresis loop closely matches the experimental results. These findings indicate that at least one discrete crack must be modeled to better approximate the experimental behavior.

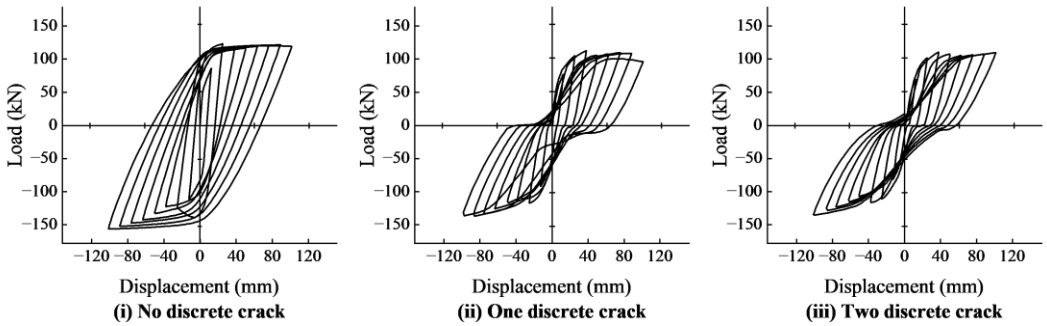

Figure 10. Hysteretic behavior of simulated beam-column with monolithic slab

The results highlight the limitations of the CDP model in representing crack-induced stiffness degradation solely through damage evolution. While CDP effectively models overall strength deterioration, it struggles to simulate localized crack opening and closing, which directly influence the pinching effect. By incorporating discrete cracks, the numerical model can better capture these critical nonlinear behaviors, improving its ability to predict experimental hysteresis responses.

Hysteresis Loop Comparison

To enable comparison between the numerical results and the experimental study by [9], the experimental hysteresis data was digitized from the published figure, as the original numerical data was unavailable. This digitization process allows for an approximate validation of the numerical model against experimental trends. The hysteresis data was initially presented in US customary units (kips and inches) and was subsequently converted to SI units (kN and mm, for consistency with the numerical simulation results. While minor inaccuracies may arise from the digitization process, this method remains a practical and widely used approach when direct access to raw experimental data is unavailable. Nevertheless, the extracted data provide a reasonable approximation of the experimental response. More importantly, the key characteristics of the hysteresis loops remain valid for comparison, ensuring meaningful validation of numerical models against experimental results.

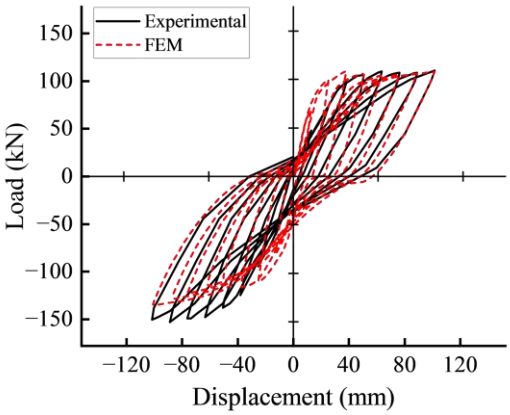

Figure 11. Comparison of hysteretic curves for experimental and simulated results

A comparison between the digitized experimental hysteresis loop and the numerical simulation results demonstrates an overall agreement in structural response, as shown in Figure 11. The numerical model successfully captures the pinching effect observed in the experimental data, resulting in a closely matching hysteresis loop shape. This indicates that the adopted modeling approach effectively represents the cyclic behavior of the RC beam-column joint. However, minor inaccuracies may arise due to parameter assumptions in the material properties.

One key factor influencing the numerical response is the use of the CDP model, particularly the compression stiffness recovery parameter w_c. A comparison between w_c = 1 (perfect compression stiffness recovery) and w_c = 0.5 (partial compression stiffness recovery) is presented in Figure 12. The value of w_c significantly affects the stiffness degradation under tension-compression reversal, where a lower w_c value results in reduced compression stiffness recovery after crack closure. As seen in Figure 12, the stiffness slope for w_c = 1 is steeper than for w_c = 0.5, indicating that lower recovery leads to greater stiffness degradation.

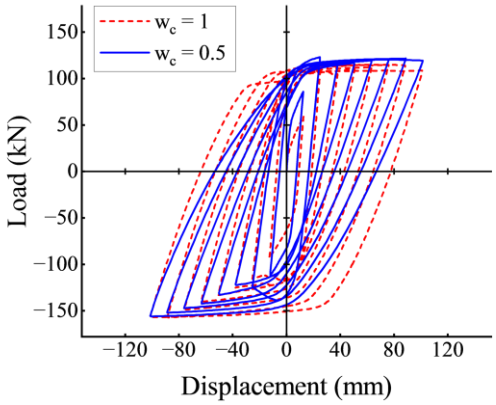

Figure 12. Comparison between w_c = 1 and w_c = 0.5 in model without discrete cracks

In addition, the reinforcement behavior is represented using a combined hardening model. In the initial loading cycles, isotropic hardening dominates, as indicated by a significant increase in strength. However, in subsequent cycles, kinematic hardening becomes dominant, characterized by the translation of the hysteresis loop without a substantial change in strength, as clearly shown in Figure 11. The minor discrepancies between the numerical and experimental results may stem from the limited availability of experimental data for these hardening parameters. In this study, values were adopted from the closest available experimental research [18], which may introduce some deviations in the simulated response.

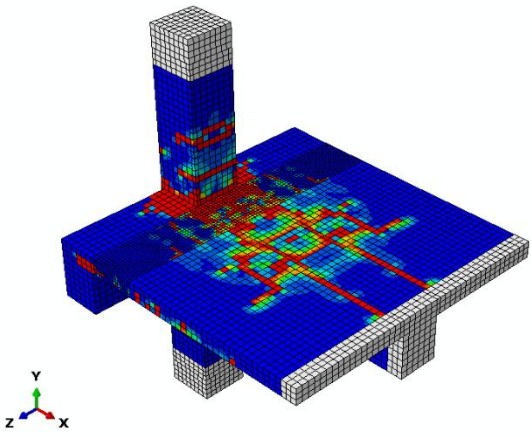

Figure 13. Tension damage representation

Overall, the numerical model successfully replicates the experimental hysteresis response, particularly in capturing the pinching effect and stiffness degradation. However, the accuracy of the results depends on the appropriate selection of material parameters, particularly in the CDP and combined hardening models. Further refinement of these parameters using experimental calibration could enhance the precision of numerical predictions.

Damage Representation

The damage model indicates that tension damage primarily accumulates at the beam-column joint, as shown in Figure 13, suggesting a high likelihood of crack formation in this region. At the end of the sixth cycle, flexural cracks develop on the column near the upper and lower region of the joint, aligning with the experimental findings [9], as shown in Figure 14. Furthermore, the accumulated tension damage in the column region of the beam-column joint indicates that this area experienced significant damage, consistent with experimental observations where the joint cover had separated. The crack pattern closely mirrors the experimental observations, with damage concentrated at the beam-column interface and diagonal cracks forming in the transverse beams due to torsional effects. This consistency with experimental results reinforces the accuracy of the numerical model in capturing the structural response under cyclic loading.

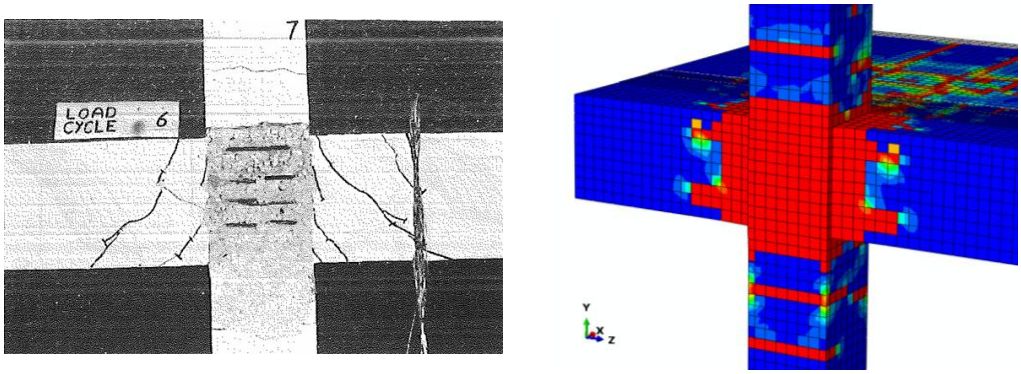

(a) Experimental (Durrani & Zerbe, 1987) (b) Simulation result

Figure 14. Beam-column joint cracks at the end of sixth cycle

Computational Efficiency

Without parallel processing, the simulations required 10.49 hours, 9.10 hours, and 9.30 hours for the models without discrete cracks, with one discrete crack, and with two discrete cracks, respectively, resulting in a total running time of 28.89 hours. The increased computation time is primarily due to the finer mesh modeled in the beam near the column face. To improve efficiency and reduce simulation time, parallel processing is recommended.

Model Limitations

In the absence of experimental data for material behavior, constitutive models can be used to define the stress-strain relationship for concrete, while reinforcement material properties can be adopted from previous studies with the closest relation to the model. Although this approach may introduce minor inaccuracies, it remains acceptable for approximating the hysteresis behavior of the structure. Additionally, while the discrete crack method effectively captures primary crack opening and closing, it does not account for minor cracks, which may contribute to additional damage and stiffness degradation.

CONCLUSION

The proposed model effectively captures the hysteresis response of RC beam-column joints with monolithic slabs under cyclic loading, demonstrating reasonable agreement with experimental results, as indicated by the similarity in hysteresis loops and damage patterns. Addressing limitations in existing FEM studies, the proposed model incorporates discrete crack representation to enhance the simulation of key nonlinear behaviors, such as pinching effects and stiffness degradation.

Additionally, the results demonstrate that a model without discrete cracks tends to overestimate energy dissipation, as indicated by a more rounded hysteresis shape compared to the pinched hysteresis observed in models incorporating discrete cracks. Incorporating at least one discrete crack significantly improves the model's accuracy, with the highest agreement with experimental results achieved when two discrete cracks are included. While the discrete crack method effectively captures primary crack behavior, it does not account for minor cracks that contribute to further stiffness degradation. The results also highlight the influence of material modeling approaches. The stiffness recovery parameter (w_c) in the CDP model directly affects compression stiffness degradation, while the combined hardening model influences the hysteresis loop evolution. Despite minor discrepancies due to parameter assumptions, the numerical model successfully represents the hysteresis behavior observed in experimental results, reinforcing its reliability for seismic performance assessment. This study advances numerical methodologies for seismic performance evaluation, bridging the gap between experimental observations and numerical modeling. Future studies should focus on refining material parameters through experimental validation and optimizing computational efficiency through parallel processing.

REFERENCES

[1]. Alfarah, B., López-Almansa, F., & Oller, S. (2017). New Methodology for Calculating Damage Variables Evolution in Plastic Damage Model for RC Structures. *Engineering Structures*, *132*, 70–86. https://doi.org/https://doi.org/10.1016/j.engstruct.2016.11.022

[2]. Alfarah, B., Murcia-Delso, J., López-Almansa, F., & Oller, S. (2017). RC Structures Cyclic Behavior Simulation with a Model Integrating Plasticity, Damage, and Bond-Slip. *Earthquake Engineering and Structural Dynamics*, 1–19. https://doi.org/https://doi.org/10.1002/eqe.2974

[3]. Ali, A., Kim, D., & Cho, S. G. (2013). Modeling of Nonlinear Cyclic Load Behavior of I-shaped Composite Steel-Concrete Shear Walls of Nuclear Power Plants. *Nuclear Engineering and Technology*, *45*(1), 89–98. https://doi.org/http://dx.doi.org/10.5516/NET.09.2011.055

[4]. Alva, G. M. S., Debs, A. L. H. de C. El, & Debs, M. K. El. (2007). An Experimental Study on Cyclic Behaviour of Reinforced Concrete Connections. *Canadian Journal of Civil Engineering*, *34*, 565–575. https://doi.org/https://doi.org/10.1139/L06-164

[5]. Birtel, V., & Mark, P. (2006). Parameterised Finite Element Modelling of RC Beam Shear Failure. *2006 ABAQUS Users' Conference*, 95–108.

[6]. Chen, W. F. (1982). *Plasticity in reinforced concrete*. McGraw-Hill.

[7]. Dassault Systèmes. (2020). *SIMULIA User Assistance 2020*. Dassault Systèmes.

[8]. Diro, G. A., & Kabeta, W. F. (2020). Finite Element Analysis of Key Influence Parameters in Reinforced Concrete Exterior Beam Column Connection subjected to Lateral Loading. *European Journal of Engineering Research and Science*, *5*(6), 689–697. https://doi.org/http://dx.doi.org/10.24018/ejers.2020.5.6.1947

[9]. Durrani, A. J., & Zerbe, H. E. (1987). Seismic Resistance of R/C Exterior Connections with Floor Slab. *Journal of Structural Engineering*, *113*(8), 1850–1864. https://doi.org/https://doi.org/10.1061/(ASCE)0733-9445(1987)113:8(1850)

[10]. Goto, Y., Kumar, G. P., & Kawanishi, N. (2010). Nonlinear Finite-Element Analysis for Hysteretic Behavior of Thin-Walled Circular Steel Columns with In-Filled Concrete. *Journal of Structural Engineering*, *136*, 1413–1422. https://doi.org/https://doi.org/10.1061/(ASCE)ST.1943-541X.0000240

[11]. Goto, Y., Mizuno, K., & Prosenjit Kumar, G. (2012). Nonlinear Finite Element Analysis for Cyclic Behavior of Thin-Walled Stiffened Rectangular Steel Columns with In-Filled Concrete. *Journal of Structural Engineering*, *138*, 571–584. https://doi.org/https://doi.org/10.1061/(ASCE)ST.1943-541X.0000504

pISSN 2302-4240
eISSN 2655-2086
Volume 14, Issue 4, December 2025, pp.01273-01285
DOI: http://dx.doi.org/10.32832/astonjadro.v14i4.19246 http://ejournal.uika-bogor.ac.id/index.php/ASTONJADRO

[12]. Kalogeropoulos, G., Tsonos, A.-D., & Iakovidis, P. (2024). Hysteresis Behavior of RC Beam–Column Joints of Existing Substandard RC Structures Subjected to Seismic Loading–Experimental and Analytical Investigation. *Buildings*, *14*(6), 1609. https://doi.org/https://doi.org/10.3390/buildings14061609

[13]. Kupfer, H., & Gerstle, K. H. (1973). Behavior of Concrete under Biaxial Stresses. *Journal of the Engineering Mechanics Division*, *99*(4). https://doi.org/https://doi.org/10.1061/JMCEA3.0001789

[14]. Lee, J., & Fenves, G. L. (1998). Plastic-Damage Model for Cyclic Loading of Concrete Structures. *Journal of Engineering Mechanics*, *124*(8), 892–900. https://doi.org/https://doi.org/10.1061/(ASCE)0733-9399(1998)124:8(892)

[15]. Li, C., Hao, H., & Bi, K. (2017). Numerical Study on the Seismic Performance of Precast Segmental Concrete Columns under Cyclic Loading. *Engineering Structures*, *148*, 373–386. https://doi.org/10.1016/j.engstruct.2017.06.062

[16]. Lubliner, J., Oliver, J., Oller, S., & Oñate, E. (1989). A Plastic-Damage Model for Concrete. *International Journal of Solids and Structures*, *25*(3), 299–326. https://doi.org/https://doi.org/10.1016/0020-7683(89)90050-4

[17]. Mander, J. B., Priestley, M. J. N., & Park, R. (1988). Theoretical Stress-Strain Model for Confined Concrete. *Journal of Structural Engineering*, *114*(8), 1804–1826. https://doi.org/https://doi.org/10.1061/(ASCE)0733-9445(1988)114:8(1804)

[18]. Narendra, P. V. R., Prasad, K., Krishna, E. H., Kumar, V., & Singh, K. D. (2019). Low-Cycle-Fatigue (LCF) behavior and cyclic plasticity modeling of E250A mild steel. *Structures*, *20*, 594–606. https://doi.org/10.1016/j.istruc.2019.06.014

[19]. Sabah, H. A. H., & Harba, I. S. I. (2022). Numerical Analysis of Reinforced Concrete Exterior Beam-Column Joints Under Limited Cycles of Repeated Loading. *Diyala Journal of Engineering Sciences*, *15*(4), 108–129. https://doi.org/https://doi.org/10.24237/djes.2022.15410

[20]. Silva, L. M. e, Christoforo, A. L., & Carvalho, R. C. (2021). Calibration of Concrete Damaged Plasticity Model Parameters for Shear Walls. *Revista Materia*, *26*(1). https://doi.org/https://doi.org/10.1590/s1517-707620210001.1244

[21]. Wang, J.-J., Liu, C., Fan, J.-S., Hajjar, J. F., & Nie, X. (2019). Triaxial Concrete Constitutive Model for Simulation of Composite Plate Shear Wall–Concrete Encased: THUC3. *Journal of Structural Engineering*, *145*(9), 04019088. https://doi.org/https://doi.org/10.1061/(ASCE)ST.1943-541X.0002355

[22]. Wang, J. H. (2020). Cyclic Behaviors of Reinforced Concrete Beam-Column Joints with Debonded Reinforcements and Beam Failure: Experiment and Analysis. *Bulletin of Earthquake Engineering*. https://doi.org/10.1007/s10518-020-00974-1

[23]. Yu-Hang, W., Qi, T., & Xin, N. (2017). Comparative Investigation on Influences of Concrete Material Constitutive Models on Structural Behavior. *Construction and Building Materials*, *144*, 475–483. https://doi.org/http://dx.doi.org/10.1016/j.conbuildmat.2017.03.174